
Article:
Palacios, A and Bradley, D (2020) Hydrogen generation, and its venting from nuclear reactors. Fire Safety Journal, 113. 102968. ISSN 0379-7112

https://doi.org/10.1016/j.firesaf.2020.102968

Hydrogen Generation, and its Venting from Nuclear Reactors

Adriana Palacios.[1,*],Derek Bradley [2]

[1]*Universidad de las Americas, Puebla, Department of Chemical, Food and Environmental Engineering, Puebla, Mexico.*

[2]*University of Leeds, School of Mechanical Engineering, Leeds, UK.*

**Corresponding author's email: adriana.palacios@udlap.mx*

ABSTRACT

Reactor fires and explosions are centred around the use of graphite as a neutron moderator, and the high temperature generation of hydrogen in reactions of steam and zirconium. An alternative to uncontrolled, excessive, build-up of pressure within the reactor, is the provision of a buffer vessel, within which there is permeable membrane separation of hydrogen from radioactive products. Possible rates of production of hydrogen are compared with the rates at which it might be separated and then flared in lifted jet flames, giving high burn rates. There are few data on the behaviour of H_2 flares in air cross flows, and this is synthesised from available data for other flammable gases. Destruction of hydrogen lifted jet flames by the cross flow of atmospheric air would seem to be less likely than for hydrocarbon jet flames. The H_2 relationships are different from those of the hydrocarbons, due to the higher chemical reactivity of H_2, its small laminar flame thickness, reduced air requirement, higher acoustic velocity, and minimal flame lift-off distance. Flaring with micro-tubes might be advantageous for integrating flaring with membrane hydrogen separation, whilst high mass flow rates can be achieved with large diameter flares in the lifted flame, supersonic regime.

Keywords: Hydrogen; jet flames; reactor venting; cross flow.

Nomenclature

Alphabet

A_e entrained air moles

A_L cross flow air moles

C total molar fraction of air in overall mixture, see Eq. (3)

C^* molar fraction of total air in fuel and air for maximum reactivity, see Eq. (5)

C_L molar fraction of air in fuel and air from lift-off volume, see Eq. (2)

C_L^* critical measured value of C_L for reduction in peak U_b^* by cross flow

C_p constant pressure specific heat (J/kg·K)

D pipe diameter (m)

D_o pipe external diameter (m)

f ratio of fuel to air moles in fuel-air mixture for S_L

F fuel jet moles

k thermal conductivity (W/m·K)

L flame lift-off distance (m)

$\overline{m}_c$ cross flow air mole density (moles/m^3)

$\overline{m}_j$ fuel mole density (moles/m^3)

P_a atmospheric pressure (Pa)

P_i initial stagnation pressure (Pa)

Re_c air cross flow Reynolds number, $u_c D_o/\nu_{air}$

S_L maximum laminar burning velocity of the fuel-air mixture in ambient atmosphere (m/s)

T^o temperature at inner layer of laminar flame (K), see [23]

u_c cross wind velocity (m/s)

u_j mean fuel flow velocity at the exit plane of pipe for subsonic flow. For ratios of atmospheric pressure to P_i equal to, or less than the critical pressure ratio, or choked sonic velocity after isentropic expansion from P_i (m/s)

U^* dimensionless flow number for choked and unchoked flow, $(u_j/S_L)(\delta_k/D)^{0.4}(P_i/P_a)$

U_δ^* Value in Eq. (6) $(u_j/S_L)(\nu_j/S_L D)^{0.4}(P_i/P_a)$

Greek letters

δ_k laminar flame thickness (m), $(k/C_p)_{To}/\rho_j S_L$

φ_{SL} equivalence ratio for maximum laminar burning velocity

ν kinematic viscosity, under conditions of ambient atmosphere (m^2/s)

ρ density (kg/m^3)

Subscripts

a ambient conditions

air air

b value at blow-off

c cross flow air

i initial stagnation conditions

j jet fuel

Highlights

1. Reactor fires arise from graphite oxidation, and H_2 from metal/steam reaction.
2. High H_2 generation necessitates buffer storage, before rapid lifted flame flaring.

3. Micro-tube flaring might be integrated with hydrogen membrane separation.
4. Data on H_2 cross flow flaring, is sparse, and synthesised from hydrocarbon data.
5. H_2 is more resistant to cross flow, with better flaring than hydrocarbons.

1. Introduction

The paper discusses lessons to be learned from a variety of nuclear reactor fires and explosions, summarised in Table 1. Loss of coolant and inadequate control systems have led to rapid self-heating, and the attainment of temperatures high enough to initiate other reactions. In water-cooled reactors the reaction of metals and steam can produce large amounts of hydrogen. In the case of the Calder Hall reactor, in which graphite moderates neutron energy to facilitate fission, uncontrolled Wigner energy release in the graphite can occur. The associated increase in temperature might initiate reaction between the graphite and coolant CO_2. The paper briefly reviews some of these key incidents. Their consequences are examined, including the possible removal and isolation of radioactive products and the containment and ultimate flaring of hydrogen in the atmosphere. This includes their possible burn rates and analyses of possible cross winds. Existing cross wind experimental data for hydrocarbons are analysed, taking into account both cross wind and jet-entrained air. In the absence of similar data for H_2, the generalised hydrocarbon findings are applied to this fuel. These ultimately suggest that H_2 flares could be more robust than hydrocarbon flares in resisting cross winds.

Table 1. Some key nuclear reactor fires and explosions.

Incident	Problem	Consequence
1957 Kyshtym. Plutonium Production. Cooling of highly radioactive waste with toxic chemicals failed.	Radioactive self-heating of liquid waste to 350 °C, in storage tank. Explosion in tank.	70-80 tonnes of radio-active waste widely dispersed in explosion.
1957 Windscale. Plutonium Production. Graphite moderated, air cooling, graphite fire.	Temp. > 380 °C during Wigner release. Metal melted. Fire increased by increased air flow.	Fire further increased by CO_2. Water risked H_2 generation, but "If it goes up, we all go with it".
1979 Three Mile Island. Pressurised Water Reactors (PWR), loss of coolant.	Core melted. Zircalloy and steam generated H_2 bubbles at top of reactor.	Hydrogen bubbles, at top released in stages, then mixed with air.

1986 Chernobyl. Boiling Water Reactors (BWR). Graphite moderator. Cooling by He/N_2. Uncontrolled rising temperature. Steam bubble increases reactivity.	Zirconium/steam generated H_2. Steam explosion probably followed by hydrogen explosion.	Excessive over-pressure destroyed reactor. Extensive fires combatted with water.
2011 Fukushima. BWR. Coolant failure due to earthquake and tsunami.	Hot zirconium cladding reacted with steam after water level dropped, producing H_2. 3 reactors had meltdowns and 1 building destroyed.	All 4 reactors had H_2 explosions. Injection of water, including seawater. Concerns about H_2 explosions.

2. General considerations

Both the 1957 Kyshtym explosion, due to radioactive overheating, and the Windscale fire just following it, arose from the production of plutonium. The Windscale reactor was graphite moderated. The high energy of nuclear irradiation creates complex interstitial loops, and vacancies, at different sites within the graphite. These effectively store differing amounts of energy. This can be released in a controlled way by heating, in what has been termed a thermal annealing process. However, if the rate of Wigner Energy release is excessive, the graphite can ignite and burn [1,2]. The Windscale fire was caused by overheating of the coolant air above 380 °C during Wigner energy release. This caused the graphite to burn in the coolant air.

During the fire, CO_2 was used in attempted fire fighting, but it increased the combustion rate. At some significant risk of excessive H_2 generation, H_2O was successfully employed [3]. Graphite moderation was also employed at Chernobyl, and in the subsequent fire, after loss of control of the reactors, the graphite became incandescent, with the formation of CO. This burned, along with the fuel cladding. Containment prior to the Chernobyl incident was inadequate. Additional difficulties are created in reactors by neutron-induced material degradation [4]. A problem with graphite, in such reactors as the Advanced Gas Cooled Reactor, is the neutron displacement damage to the graphite structure. It is difficult to replace the damaged graphite, during the reactor lifetime, although this was reportedly achieved with the St. Petersburg reactor. Corrosion rates of zirconium can become 10 times greater inside a reactor [4].

Loss of coolant in the Pressurised Water Reactors at Three Mile Island resulted in the generation of H_2, principally through the reaction of steam with the zirconium of the fuel cladding. Although

there was no major breach in the containment, about half of the reactor core was melted and radio-nuclides remained inside the reactor, or were dissolved in the water. A venting system with a 100 m high stack had been provided to serve the principal containment, but this was ineffective due to the power failure. Consequently, the hydrogen was widely dispersed, albeit with the advantage of weakening the flammable mixture by dilution. On the other hand, any turbulence that was generated might have enhanced the burning rate, to the point where it even ultimately quenched some of the leaner flamelets. Subsequently, it was estimated that, for the Three Mile Island conditions, an 8% H_2 mixture was burning, with the generation of 190 kPa over-pressure [5].

The interplay of the weakening of the mixture and the turbulence was subsequently confirmed in a study of the turbulent combustion of H_2/air mixtures, sponsored by the UK Atomic Energy Authority. Some results are shown in Fig. 1, in the form of plots of flame speed for mixtures of 6, 8 and 10% H_2 with air, against rms turbulent velocities [6]. The stoichiometric proportion is 29.6%. The measurements were of explosive burning in a fan-stirred containment vessel. Initially, turbulent flame wrinkling increased the flame speed, but at the higher rms velocities, the turbulence was strong enough to create stretch extinctions of some of the leaner flamelets.

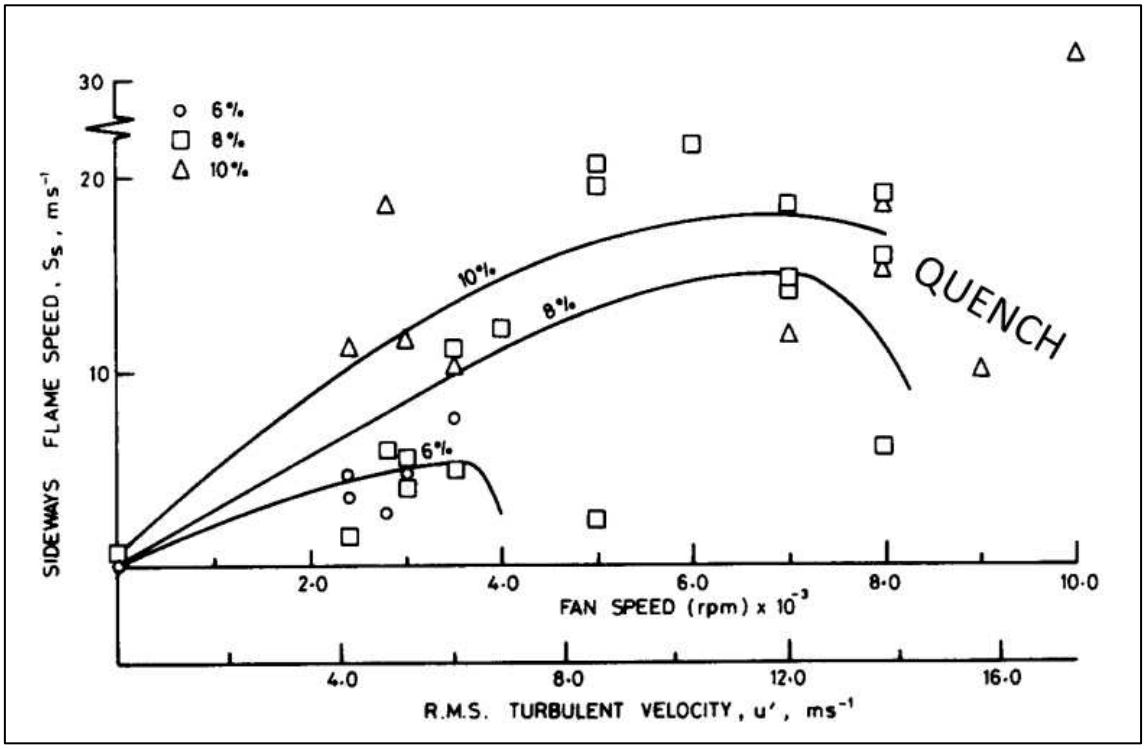

Fig. 1. Quenching effect of the rms turbulent velocity on hydrogen/air flame speed, for three different mixtures, modified from [6].

After this incident, reactor owners were required to strengthen venting systems to prevent leakage of H_2 into secondary containment buildings. Most of the H_2 was generated from zircalloy cladding reacting with steam. It has been estimated that 1,200 kg of H_2 would be created, were all the cladding to be oxidised by steam, and that complete combustion of the zirconium in a 1,000 MW(e) reactor would release $198 \cdot 10^9$ Joules [4].

Hydrogen and O_2 can also be formed in light water cooled nuclear reactors by the radiolytic decomposition of water [7]. If significant amounts of H_2 and O_2 were to be created by radiolysis in stoichiometric proportions, this would be very serious because of the very high reactivity, and the potential for detonation, of such a mixture [8]. However, Gordon et al. [9] found this not to be so, with no more than 0.7% H_2 being created by radiolysis, which could be removed by recombination. To avoid explosive recombination with O_2, many reactors have been retrofitted with passive hydrogen re-combiners within the containment. Other remedial action has involved injection of N_2 into the reactor.

One approach, implemented in a few Boiling Water Reactors, has been to burn the H_2 inside the containment using distributed glow plugs [10]. H_2/steam/air modes of reaction, ranging from mild deflagration to detonation, have been studied computationally in Russia. Details of mathematically modelled reaction fronts within the containment of the reactor are given in [11].

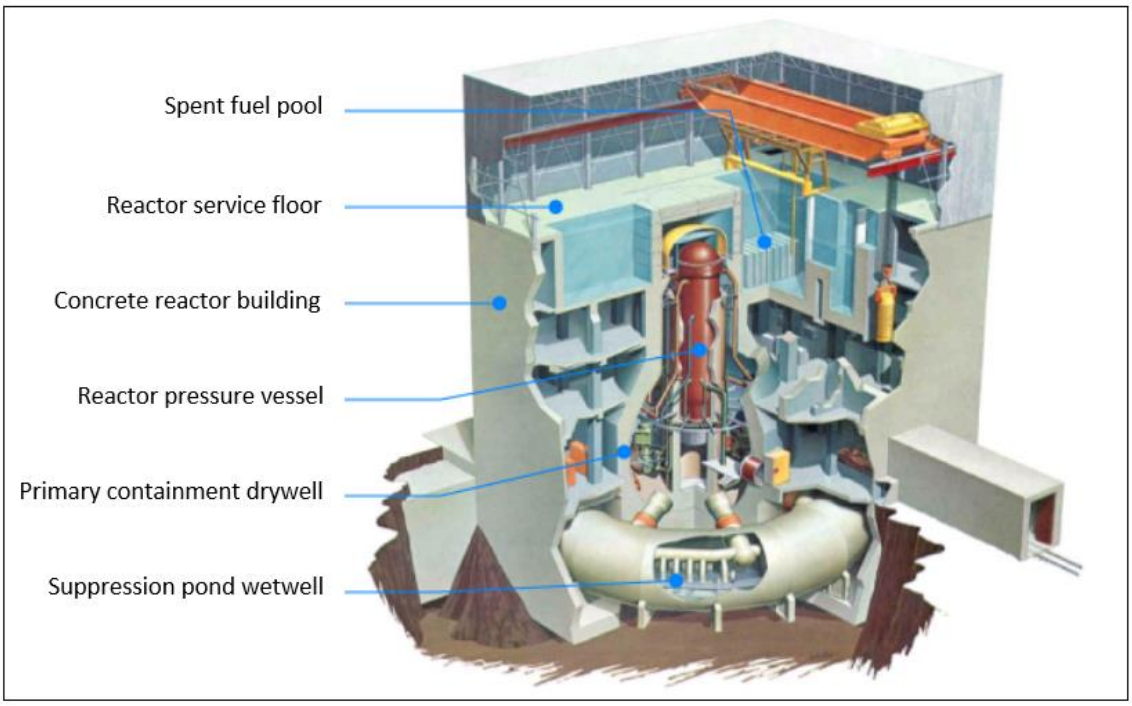

Fig. 2. Containment of Reactor Pressure Vessel, taken from [12].

At Fukushima, reactors survived the earthquake, but less so the tsunami. There was no reactor cooling an hour after shut down. At both Three Mile Island and Fukushima there were failures to remove the radioactive decay heat from the fuel [12]. At Fukushima all the fuel in Unit 1 melted, with much of it leaking out. Seawater, with neutron absorbing boron, were used as coolant, but reactors overheated for many days. The reactors were GE/Toshiba/Hitachi Boiling Water Reactors, operational since 1971-75, with powers ranging from 460 to 1,784 MW(e). Pressure built up in Units 1 to 3, with most of the fuel melting [12]. Venting was designed to be through an external stack, but, in the absence of power, most of the gas back-flowed into the top floor of the reactor building. Venting began almost 24 hours into the emergency [13]. Containments were vented to atmosphere. Hydrogen leaked into reactor buildings and caused large explosions in Units 1, 3 and 4. Each Unit was estimated to have produced 800-1,000 kg of H_2. Hydrogen explosions caused tremendous damage. Even when fissioning had ceased, significant heat was generated through radioactive decay.

As a consequence, the three Fukushima reactor cores, see Fig. 2, melted in the first two or three days of the emergency. There were considerable releases of radio nuclides and cooling water,

with a total of ten core melts. The rate of formation of H_2 was controlled by the rate of oxidation of the zirconium fuel cladding by steam, at about 1,300 °C [7]. This rate of reaction was far beyond the capability of H_2 recombiners, N_2 inerting, and the time required to ensure the requisite purity of vented gases. These complexities pose the current major challenge.

3. The challenge

In a loss of coolant, or similar crisis, the reactor and its immediate containment are of inadequate volume to contain all the hydrogen that might be generated. This is evident from the relatively small Primary Reactor Containment shown in Fig. 2. Boiling Water Reactors operate at pressures of about 8 MPa, while Pressurised Water Reactors, with a secondary circuit, operate at about 16 MPa. If venting were to be long-delayed, then a worse situation would arise from the failure of the reactor/containment. Yet, unless it is well controlled, allowing emergency venting to atmosphere to occur too early would disperse undesirable radio-nuclides. It would also increase the probability of uncontrolled hydrogen explosions. This perspective leads to the necessity of a large buffer vessel, into which the primary products could be vented from the reactor. Ultimately, large amounts of H_2 must be vented, preferably free of the undesirable radio-active products. This could be achieved by separating and then containing such products, while the hydrogen would be contained, and ultimately flared in a controlled manner.

Hydrogen separation has been proposed, possibly through the use of permeable membrane separators, operating in a stream rich in H_2. This also could be passed through charcoal adsorbers to remove radio-active particles, and then flared in a gas burner [14,15]. Inability to control the build-up of the high temperature reaction products, inadequate venting rates, particularly of hydrogen, and crisis management, have been characteristic features of the described malfunctions. An essential requirement is a large buffering volume to contain the products during their initial high rates of formation. It is also desirable to separate and contain the most damaging products, whilst flaring hydrogen as soon as possible, in order to prevent its build up. A safe balance must be sought, between rates of H_2 production, storage, separation, and flaring.

Although the flaring of vented H_2 is not essential, the venting must prevent its hazardous flammable accumulation elsewhere. In the absence of flaring, a large number of small diameter

pipes would be necessary to ensure quenching of any potential flame. Careful design would also be necessary to avoid any subsequent accumulation of H_2 in flammable concentrations in other regions. The hydrogen flaring process is now briefly considered, in terms of its feasibility for achieving adequate burn rates, the practicality of flaring, including the ability of flares to withstand cross winds.

4. Control of hydrogen flaring: limitations due to blow-off

Jet flames exhibit a variety of structures, ranging from those comprised of lifted flames, which have the highest burn rates, to flames with air cross flow that can create rim and wake-stabilised flames. At sufficiently high flow rates, the last are stabilised by the wake of the strong air flow across the fuel pipe. In lifted flames, blow-offs and extinctions can occur at sufficiently high values of the fuel flow number, U^*, and low values of the pipe diameter, D, normalised by δ_k, the flame thickness, at the maximum laminar burning velocity, S_L. The wake-stabilised flames can blow-off when the Reynolds number, Re_c, becomes sufficiently high [16].

Because of the importance of their higher burn rate, lifted flames, with and without cross flow, will be considered in greater detail than in the earlier analysis in [17]. The flow number at blow-off, U_b^*, was formulated on the basis of both stretched laminar flamelet mathematical modelling [18,19], and the experimental derivation, correlation, and validation of appropriate dimensionless groups. Data were drawn from a vast experimental data bank [19]. This covered jet velocities, burning velocities, emitting plume heights, flame lift-off distances, flame heights, and six different fuels.

Flaring consists of the burning of a jet of excess fuel in the atmosphere. The highest burn rate within the reaction zone, was found to occur at the leading edge if the lifted flame, with flamelets burning at the maximum laminar burning velocity, at an associated localised equivalence ratio of φ_{SL} [18]. The lift-off distance, L, is the distance between the exit plane of the pipe and this leading edge. If the ratio, D/δ_k, [18] is small, air dilution rapidly occurs, there is difficulty in maintaining combustion, and the flame is soon quenched by excessive air entrainment.

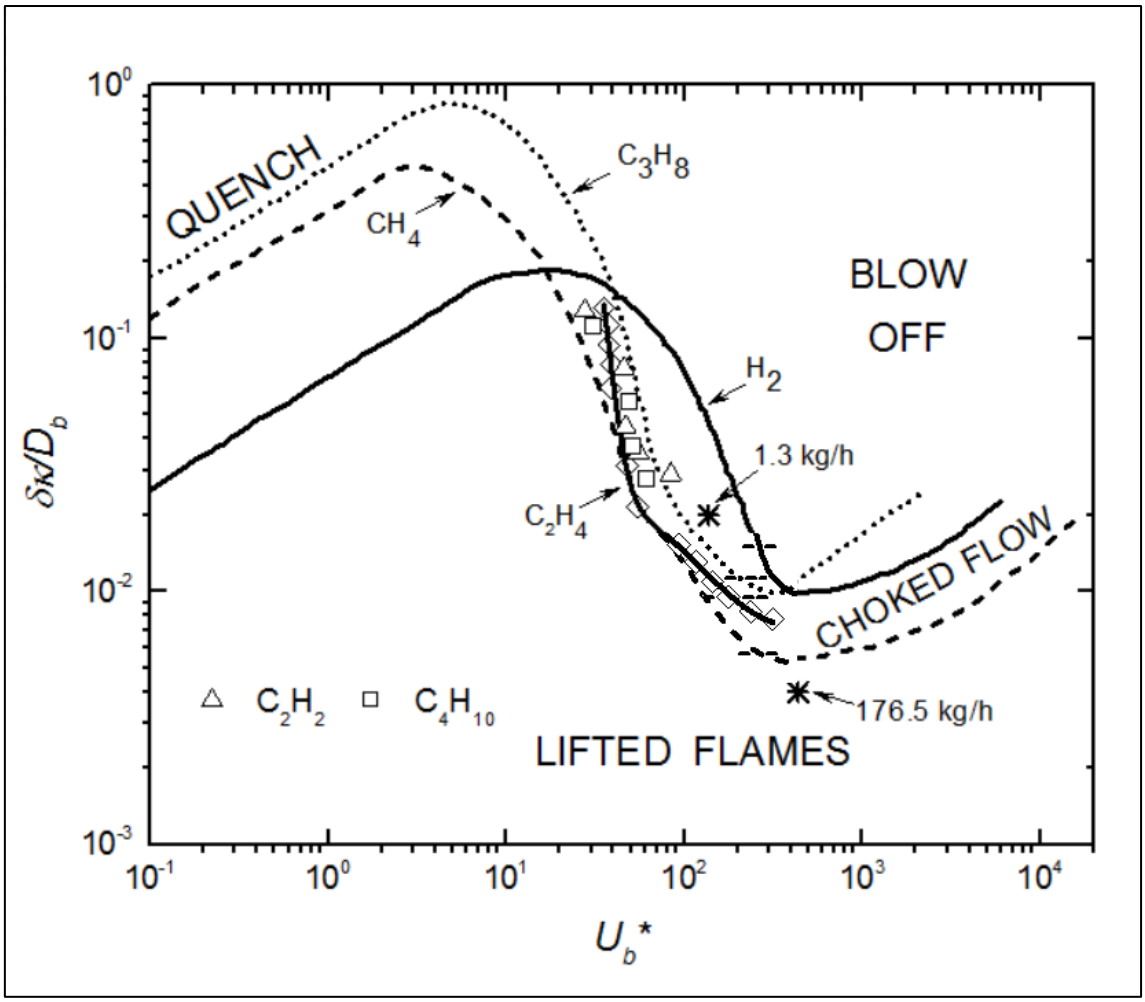

Fig. 3. Sonic and subsonic lifted jet flame blow-off and quench boundaries, for C_3H_8, CH_4, H_2 and C_2H_4, with more limited data for C_2H_2 and C_4H_{10}. Short dashed horizontal lines on complete curves show critical pressure ratio conditions.

Figure 3 shows the experimentally based correlations of the dimensionless flow number, U_b*, for lifted flames at blow-off. There are no cross flows, and data are shown principally, for C_3H_8, CH_4, C_2H_4 and H_2. More limited data also appear for C_2H_2 and C_4H_{10}. The blow-off flow number is defined as $U_b^* = (u_j/S_L)(\delta_k/_b)^{0.4}(P_i/P_a)$, where u_j is the mean fuel exit velocity, D_b the pipe diameter for blow-off, and (P_i/P_a) the ratio of upstream stagnation to atmospheric pressure.

Uniquely, in H_2 flames, the high diffusivity of H atoms induces significant heat release earlier in the flame [21]. This necessitates a different generalised approach in the use of flame thickness in correlations, [22]. The flame thickness is given by $\delta_k = (k/C_p)_{To}/\rho_j S_L$ [23], with T^o the inner layer temperature. The data in Fig. 3 are experimentally based, taken from [22], except for C_2H_4 taken

from [24], and are overwhelmingly from the subsonic, pre-choked, regime. Values of δ_k are for the maximum laminar burning velocity at the leading flame front.

Locations at which the critical pressure ratio is attained on each complete blow-off curve in Fig. 3 were found from the compatibility of δ_k/D_b and U_b* at this pressure ratio. These are indicated by the short horizontal broken lines, below which flow is choked at blow-off. Below the blow-off curve, U_b*, for a given fuel, towards the lower values of δ_k/D_b, is the regime of lifted flames, with increasing pipe diameters. Above the blow-off curve, towards the higher values of δ_k/D_b is the regime of blow-off, with decreasing pipe diameters. It is clear from Fig. 3 that, within the subsonic regime, as δ_k/D decreases, the range of possible stable U* values is narrowed.

Some contrasting flow rates for hydrogen flaring, with S_L = 3.03 m/s, are now analysed, in terms of these generalised characteristics of lifted jet flames. First, in Fig. 3 the use of a micro-tube, D = 2.0 mm, δ_k = 0.03985 mm [22, 23], δ_k/D_b = 0.02, is considered. The initial/atmospheric pressure ratio is P_i/P_a = 1.8, just within the subsonic regime, before choked flow develops. Because of the high acoustic velocity of H_2, arising from the low molecular mass, the exit velocity, u_j, is also high, at 1,159 m/s, and U_b* = 144. These conditions give a micro-tube mass flow rate of H_2 of 1.3 kg/hour, indicated by the upper asterisk in Fig. 3.

In contrast, now consider blow-off in the choked flow regime, with P_i/P_a increased to 10 and D = 10 mm. In this regime, the reaction rate is enhanced by shocks and supersonic flows, at high U_b*. Now δ_k/D_b = 0.004, and u is equal to the acoustic velocity of 1,202 m/s, with an associated density of 0.519 kg/m^3. These conditions yield U_b* = 436, a mass flow rate of 176.5 kg/hour, indicated by the lower asterisk on the figure, and a jet flame heat release rate of 6.9 MW. The generalised data in [20] suggest that the jet flame height would be 4.8 m.

Importantly, hydrogen has a number of rather unique characteristics contributing to high jet velocity flames: a high laminar burning velocity, small flame thickness, small air requirement, and a high acoustic velocity. In contrast, its high reactivity makes it more prone to flame flashback in premixed systems.

5. Effects of air cross flow

5.1 Hydrocarbon flames in cross flow

An important characteristic that is required in the flared venting of lifted jet flames, is an ability to survive extinction in atmospheric cross winds, perpendicular to the jet. Available experimental data, on the effect of cross winds on U_b* have been re-expressed, but for pre-choked flow only, in terms of an air cross flow parameter, C_L. This is the mole fraction of cross flow air in the mixture with jet fuel, created within the lift off distance, L. This has a volume $(\pi D^2/4)L$, with measured steady fuel jet and air cross flows into it. The mole ratio of jet fuel to air cross flow, F/A_L, with respective fuel and air velocities, u_j and u_c, into the lift-off volume, is given by:

$$F/A_L = (u_j\overline{m}_j/u_c\overline{m}_c)\pi/4(D/L), \quad (1)$$

and the mole fraction of air in this fuel/air mixture is:

$$C_L = A_L/(A_L + F) = (1 + F/A_L)^{-1}. \quad (2)$$

Several researchers have shown that there is good mixing of the fuel jet and transverse air flow [24-27]. Experimental studies have shown the effects of cross flows on lifted jet flames. These data have been processed to give blow-off data, U_b*, in terms of C_L and the normalised pipe diameter, D/δ_k. Data were taken for C_3H_8, CH_4, and C_2H_4, with D/δ_k within the comparatively narrow range of 32–62, from part of Kalghatgi's study in [24]. For the necessary L/D lift-off data, generalised expressions containing L/D for the different fuels as a function of U*, were taken from [20]. These expressions have recently received further experimental confirmation by Z. Wang et al. [28].

The values of U* and C_L derived in this way are shown for the three hydrocarbons in Fig. 4. Peninsulas of flame stability are created, over ranges of U* and C_L, for particular values of D/δ_k. Decreases in D/δ_k, narrow the ranges of possible stable U* and C_L values, with an increasing tendency for flame quenching by excesssive entrainment. For all the peninsulas in Fig. 4, blow-off occurs at the upper, lifted flame limit, U_b*. For larger diameter burners, the flames are more stable, deeper into the lifted flame regime. As the air cross flow velocity, u_c, and C_L increase from zero, the value of U_b* at the upper lifted flame limit also initially increases, and the mixture within the lift-off volume becomes progressively more reactive.

It is interesting to compare this aeration with that when air is added to the fuel within the supply pipe [29]. In that case U_b* decreased as the amount of air increased, because fuel was removed to be replaced by air, whereas with cross flow the air does not reduce the fuel supply.

However, increasing cross flow dilution eventually decreases the reaction rate, and it becomes impossible to sustain a high value of U_b* without an increase in D/δ_k. Flame survival at a relatively high value of C_L can then only be achieved by a sharp reduction in U* and the reaction rate, together with some decrease in C_L.

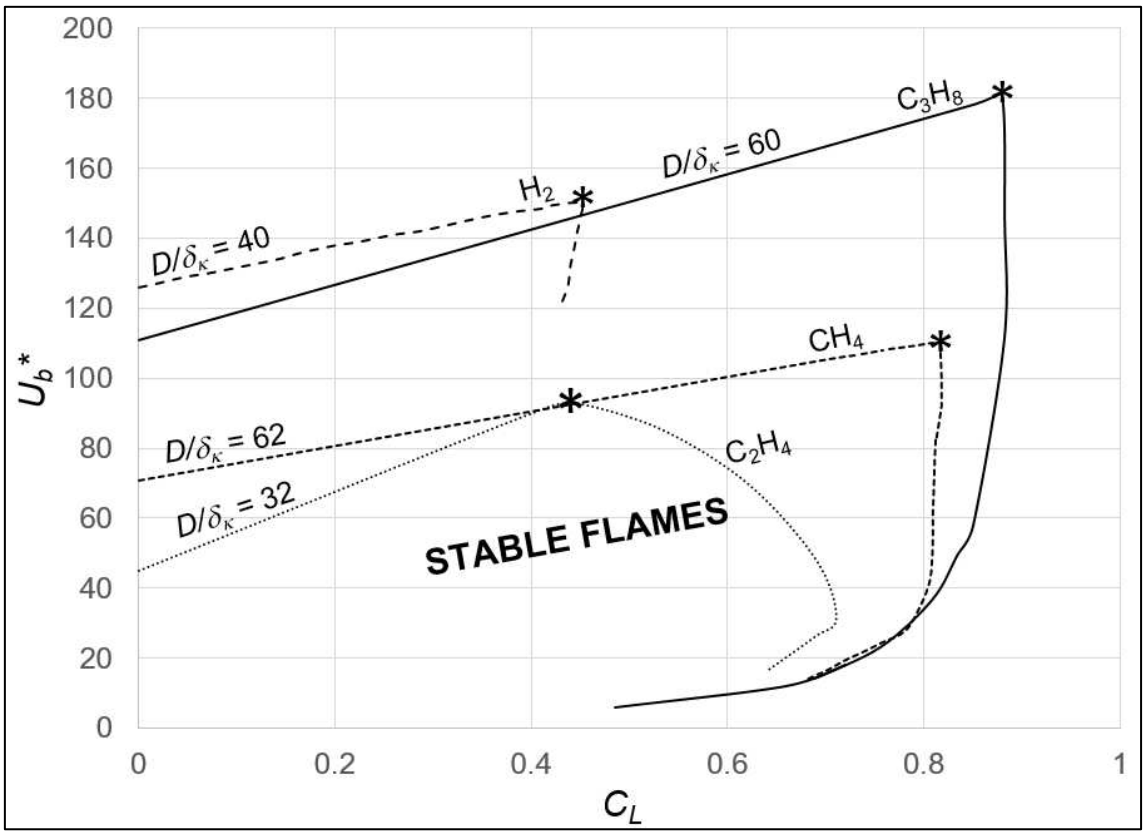

Fig. 4. Blow-off limits of stable CH_4, C_2H_4 and C_3H_8, lifted flames with air cross flows, in terms of U_b* versus C_L, for different values of D/δ_k. The dashed curve for H_2 is synthesised from the data of the other fuels, * indicates values of C_L* for all the fuels.

The experimental values of C_L at the onset of the sharp falls in U_b*, namely C_L*, are listed in Table 2, and are indicated by * in Fig. 4. At lower values of U* below U_b*, there is an intermediate regime of stable, rim-attached, never-lift, severely bent, flames, that have been well characterised by Huang and Chang in [34]. Ultimately, values of U* decrease to the lowest limit, at which flames can be stabilised, with wake induced flows and downwash [24]. These have ceased to be

lifted flames. For Re_c > 3,000, a downwash-attached, wake flame could be generated, but its value of U^* would be significantly lower than that of a lifted jet flame [35].

In the present study of venting flames, only the early stages of lifted flame quenching, at the higher values of U^*, are relevant. The C_2H_4 plot in Fig. 4 demonstrates the effects of the increasing flame quenching that occur with decreasing of D/δ_k at its lower values, in this case one of 32.

To characterise the fuel/air mixture more completely, allowance must be made for the atmospheric air, A_e, that is entrained by the jet. The total molar fraction of air in the overall mixture, C, is then defined by:

$$C = (A_L + A_e)/(A_L + A_e + F) = [1 + F/(A_L + A_e)]^{-1}. \quad (3)$$

A further important factor controlling lifted jet flames in cross flows, is the ratio, f, of fuel to air moles for the most reactive equivalence ratio, φ_{SL}, at the jet flame leading edge. It also appears in expressions for flame lift-off distance. For the most reactive mixture composition, C, is given by C^*. From Eq. (3):

$$F/(A_L + A_e) = f, \text{ and} \quad (4)$$

$$C^* = [1 + f]^{-1}. \quad (5)$$

Values of f, φ_{SL}, S_L, and C^*, for the conditions of Fig. 4, are given in Table 2. Hydrogen requires significantly less air than hydrocarbons, with the value of f for H_2 more than ten times higher than that for C_3H_8.

Table 2. Property values and references for characterising Fig. 4.

Fuel	D/δ_k	Ref. S_L	φ_{SL}	S_L, m/s	f	C^*	C_L^*
C_3H_8	60	[30]	1.1	0.43	0.046	0.96	0.88
C_2H_4	32	[31]	1.2	0.72	0.084	0.92	0.44
CH_4	62	[32]	1.02	0.39	0.107	0.903	0.82
H_2	40	[33]	1.8	3.03	0.756	0.57	(0.45)

The maximum rate of burning will be at, or close to, the asterisked points in Fig. 4. In terms of C_L, this will be C_L^*, and in terms of C it is C^*.

The maxima experimental values of C_L in Fig. 4, C_L^*, will always be smaller than those of C^*. This is because of the exclusion of the jet-entrained air in the evaluation of C_L. The amount of

such air always exceeds that of the cross flow air in all the present cases. In addition, there is also the possibility that not all the cross flow mixes with the fuel. Nevertheless, the theoretically based values of C^* are a guide to the more practical values of C_L^*.

5.2 Hydrogen flames in cross flow

Unfortunately, no relevant cross wind data could be found for H_2. These, had to be generated from the data on U_b^* and the cross flows from the hydrocarbon experiments. The value of $C^* = 0.57$ for H_2, suggested a synthesised "experimental" value of C_L^* of 0.45, in the light of such considerations. In the absence of cross flow, with $D/\delta_k = 40$, the experimental data suggest $U_b^* = 126$ [22], with $P_i/P_a = 1.6$. If it is assumed that the changes in U_b^* are similar to those for C_3H_8, then at $C_L^* = 0.45$, $U_b^* = 150$, with $P_i/P_a = 1.75$. These data, together with the experimental value of U_b^* of 126, without a cross wind for H_2, enabled the dashed blow-off characteristic curve in Fig. 4 to be constructed, bearing in mind that, for the necessary lifted flames, only the upper part of the U^* versus C_L relationship is necessary.

An important practical consideration is whether a hydrogen flare could endure the prevailing cross winds. With the synthesised value of C_L^* of 0.45 in Eq. (2), the value of F/A_L is 1.22, for the mixture leaving the lift-off zone. Provided D/L can be evaluated in Eq. (1), it is possible to establish the practically important cross flow velocity, u_c. The expression for the normalised flame lift-off distance in [36] makes solution possible, albeit based on a different expression for laminar flame thickness in U_δ^*:

$$(L/D)f = -0.0002U_\delta^{*2} + 0.19U_\delta^* - 3.3. \qquad (6)$$

For the synthesised H_2 quench conditions in Fig. 4 of $U_b^* = 150$, $u_j = 1131$ m/s, $D/\delta_k = 40$, $f = 0.756$, then $u_c = 51$ m/s. A natural atmospheric cross wind as high as this is uncommon. It is therefore unlikely that a lifted, venting hydrogen flame could be significantly disturbed by atmospheric conditions, and make the transition to a slower burning attached flame. Furthermore, any smaller cross flow would enhance U_b^* and u_j.

This behaviour contrasts with that for C_3H_8 and CH_4. For the C_3H_8 peninsula in Fig. 4, the experimental data show quenching to begin at $u_j = 242$ m/s, with $u_c = 5$ m/s, as U_b^* begins to fall sharply. For the CH_4 peninsula, comparable values are $u_j = 192$ m/s and $u_c = 3$ m/s. These low

values of u_c suggest that, for these fuels, quite moderate cross flows can jeopardise the stability and burning rate of lifted flames. The high value of f for hydrogen reduces the air requirement and lift-off distance, while the high acoustic velocity is associated with high jet velocities at a given Mach number. These can be subsonic, yet in excess of 1,000 m/s.

This demonstration of the synthesis of cross flow characteristics is based on a low value of D/δ_k. Larger values could have been chosen. In un-choked flow, H_2 lifted jet flames are possible over greater ranges of conditions than other fuels. For lifted flames, an increase in U^* must in general be matched with an increase in D/δ_k.

6. Conclusions

1. Loss of coolant and other malfunctions can result in reactors over-heating and creating a variety of chemical reactions and heat releases. These aspects must also be under continuous review, in the context of the continuing desire and social pressure to improve the efficiency of power generation by operating reactors at higher temperatures. Unacceptable consequences would be uncontrolled reactor failures, with the release of radioactive products and explosive gases into the atmosphere. Ideally, such a release could be avoided by early venting of the reactor, without any release of noxious products and flammable gases, and no external explosion. This might be achieved by initially venting the reactor into much larger buffer vessels, in which the hydrogen might be wholly or partially separated and then flared.

2. In normal operation, H_2 re-combiners can process about 195 kg/hr of H_2, but in the case of an accident, the required rate would have to increase 100 to 400 fold [14], well beyond the capabilities of this technique. In this situation, it has been proposed that, after removal of the water from the gaseous mixture, the H_2 should be separated, using a gas permeable membrane separator [14]. The H_2 stream would then pass through a charcoal adsorber to remove radioactive products, before being finally flared. If choked flow flaring on a 10 mm pipe, as demonstrated in Fig. 3 at a rate of 176.5 kg/hr, were to be employed, the accumulated approximate estimate of 3,000 kg of H_2 produced at Fukushima would be flared on three such burners in just under 6 hours. There are a variety of possible ways in which H_2 membrane separation might be implemented, covering a rich variety of materials, and structures [37].

3. With hydrogen permeable membrane separation, it is suggested in [14] that the differential pressure across the membranes should not exceed 1.72 MPa. As an example, if the H_2 were to be stored at 2 MPa and 300 K, 1,000 kg of H_2 would occupy a volume of 1,638 m^3, a cube with a 11.8 m side. This is a practically convenient size, that might combine storage and separation facilities. The present analyses of the subsequent flaring have shown that the characteristics of H_2 are particularly well suited to a flexible approach to storage, separation and flaring, albeit with some possible delay for H_2 separation if dispersal of harmful radio-active products is to be avoided.

4. Flaring of H_2 is favoured by its low air requirements which lead to compact lifted flames. Its high acoustic velocities, arising from its low molecular mass, combined with its high burning velocity, lead to high values of fuel jet velocity. Although the analysis of air cross flow on H_2 lifted flames provides only an estimate of velocities, rather than accurate predictions, it nevertheless clearly shows that the extinction of lifted flames due to atmospheric cross winds is unlikely. The same cannot be said of C_3H_8 and CH_4 flames. There is clearly a need for experimental data on H_2 lifted jet flames in cross flows.

5. A unique aspect of H_2 jet flames is their ability to support micro-jet flames, a consequence of their low δ_k values. This could be relevant also in the separation process. Another possibility is for the vented gas from the reactor to be immediately flared in a bank of micro-jets, followed by removal of radio-nuclides.

Acknowledgements

A.P. gratefully acknowledges the financial support of the Royal Society in the form of a Newton International Fellow Alumnus.

References

[1] R.H. Telling, C.P. Ewels, A.A. El-Barbary, M.I Heggie, Wigner Defects Bridge The Graphite Gap, Nature Materials. 2 (2003) 333–337.

[2] P.C. Minshall, A.J. Wickham, The Description of Wigner Energy and Its Release From Windscale Pile Graphite for Application to Waste Packaging and Disposal (2001) International Nuclear Information System, RN32039324, International Atomic Energy Agency, IAEA-NGWM CD-01.

[3] The Windscale Inquiry, The National Archives, 1978.

[4] S.J. Zinkle, G.S. Was, Materials Challenges in Nuclear Energy, Acta Mater. 61 (2013) 735–758.

[5] H.A. Postma, Analysis of Three Mile Island (TMI-2) Hydrogen Burn, Thermal Hydraulics of Nuclear Reactors, 1983.

[6] D. Bradley, K.J. Al-Khishali, S.F. Hall, Turbulent Combustion in Near-Limit Hydrogen-Air Mixtures, Combust. Flame 54 (1983) 61–70.

[7] Safety of Nuclear Reactors, World Nuclear Association, Updated May 2016.

[8] D. Bradley, M. Shehata, Acceleration of Laminar Hydrogen/Oxygen Flames in a Tube and the Possible Onset of Detonation, Int. J. Hydrogen Energ. 43 (2018) 6734–6744.

[9] S. Gordon, K.H. Schmidt, J.R. Honekamp, An Analysis of the Hydrogen Bubble Concerns in the Three Mile Island Unit-2 Reactor Vessel, Radiat. Phys. Chem. 21 (1983) 247–258.

[10] F. Tamanini, E.A. Ural, J.L. Chaffee, Hydrogen Combustion Experiments in a 1/4 Scale Model of a Nuclear Power Plant Containment, Proc. Combust. Inst. 22 (1988) 1715–1722.

[11] V. Kotov, V. Bezlepkin, D. Kapitsa, Hydrogen Safety in Design of the Nuclear Power Plant, Proc. Ninth Int. Seminar on Fire and Explosion Hazards, Eds. A. Snegirev, N.A. Liu, F. Tamanini, D. Bradley, V. Molkov, N. Chaumeix, St. Peter the Great Polytechnic University. pp. 1259-1268 (2019).

[12] Fukushima Accident, World Nuclear Association, Updated October 2017.

[13] M. Holt, R.J. Campbell, M.B. Nikitin, Fukushima Nuclear Disaster, Congressional Research Service Report for Congress., 7–5700, 2012.

[14] V.M. Callaghan, E.P. Flynn, B.M. Pokora, Containment Hydrogen Removal System for a Nuclear Power Plant, United States Patent 4430293 (1984).

[15] Lei Wang, Cheng Shao, Hai Wang, Hong Wu, Radial Basis Function Neural Networks-Based Modeling of the Membrane Separation Process: Hydrogen Recovery from Refinery Gases, Jour. Nat. Gas Chem. 15 (2006) 230–234.

[16] M.R. Johnson, L.W, Kostiuk, Efficiencies of Low-Momentum Jet Diffusion Flames in Crosswinds, Combust. Flame 123 (2000) 189–200.

[17] A. Palacios, D. Bradley, Fires, Explosions, and Venting in Nuclear Reactors, Proc. Ninth Int. Seminar on Fire and Explosion Hazards, Eds. A. Snegirev, N.A. Liu, F. Tamanini, D. Bradley, V. Molkov, N. Chaumeix, St. Peter the Great Polytechnic University. pp. 808-817 (2019).

[18] D. Bradley, P.H. Gaskell, Xiao-Jun Gu, The Mathematical Modeling of Liftoff and Blowoff of Turbulent Non-Premixed Methane Jet Flames at High Strain Rates, Proc. Combust. Inst. 27 (1998) 1199–1206.

[19] D. Bradley, D.R. Emerson, P.H. Gaskell, Xiao-Jun Gu, Mathematical Modelling of Turbulent Non-premixed Piloted-Jet Flames with Local Extinctions, Proc. Combust. Ints. 29 (2002) 2155–2162.

[20] D. Bradley, P.H. Gaskell, Xiao-Jun Gu, A. Palacios, Jet Flame Heights, Lift-Off Distances and Mean Flame Surface Density for Extensive Ranges of Fuels and Flow Rates, Combust. Flame 164 (2016) 400–409.

[21] D. Bradley, S.E-D. Habik, S.A. El-Sherif, A Generalisation of Laminar Burning Velocities and Volumetric Heat Release Rates, Combust. Flame 87 (1991) 336–345.

[22] A. Palacios, D. Bradley, Generalised Correlations of Blow-Off and Flame Quenching for Sub-Sonic and Choked Jet Flames, Combust. Flame 185 (2017) 309–318.

[23] J. Göttgens, F. Mauss, N. Peters, Analytic Approximations of Burning Velocities and Flame Thicknesses of Lean Hydrogen, Methane, Ethylene, Ethane, Acetylene and Propane Flames, Proc. Combust. Inst. 24 (1992) 129–135.

[24] G.T. Kalghatgi, Blow-Out Stability of Gaseous Jet Diffusion Flames Part I: In Still Air, Combust. Sci. Tech. 26 (1981) 233–239.

[25] M.P Escudier, Aerodynamics of a Burning Turbulent Gas Jet in a Crossflow, Combust. Sci. Tech. 4:1 (1971) 293–301.

[26] R.W. Grout, A. Gruber, C.S. Yoo, J.H. Chen, Direct Numerical Simulation of Flame Stabilization Downstream of a Transverse Fuel Jet in Cross Flow, Proc. Combust. Inst. 33 (2011) 1629–1637.

[27] H. Kolla, R.W. Grout, A. Gruber, J.H. Chen, Mechanisms of Flame Stabilization and Blowout in a Reacting Turbulent Hydrogen Jet in Cross-Flow, Combust. Flame 159 (2012) 2755–2766.

[28] Z. Wang, K. Zhou, M. Liu, Y. Wang, X. Qin, J. Jiang, Lift-off Behavior of Horizontal Subsonic Jet Flames Impinging on a Cylindrical Surface, Proc. Ninth Int. Seminar on Fire and Explosion Hazards, Eds. A. Snegirev, N.A. Liu, F. Tamanini, D. Bradley, V. Molkov, N. Chaumeix, St. Peter the Great Polytechnic University. pp. 831-841. ISBN: 978-5-7422-6498-9.

[29] A. Palacios, D. Bradley, L. Hu, Lift-off and Blow-off of Methane and Propane Subsonic Vertical JetFlames, With and Without Diluent Air, Fuel 183 (2016) 414–419.

[30] A. Vanmaaren, L.P.H. DeGoey, Stretch and the Adiabatic Burning Velocity of Methane- and Propane-Air Flames, Combust. Sci. and Tech. 102 (1994) 309–314.

[31] T. Hirasawa, C.J. Sung, A. Joshi, Z. Yang, H. Wang, C.K. Law, Determination of Laminar Flame Speeds using Digital Particle Image Velocimetry: Binary Fuel Blends of Ethylene, Proc. Combust. Inst. 29 (2002) 1427–1434.

[32] Xiao-Jun Gu, M.Z. Haq, M. Lawes, R. Wooley, Laminar Burning Velocity and Markstein Lengths of Methane–Air Mixtures, Combust. Flame 121 (2000) 41–58.

[33] C.J. Sun, Chih-Jeng Sung, Longting He, Chung-King Law, Dynamics of Weakly Stretched Flames: Quantitative Description and Extraction of Global Flame Parameters, Combust. Flame 118 (1999) 108–128.

[34] Rong-F. Huang, Jean-M. Chang, The stability and Visualized Flame and Flow Structures of a Combusting Jet in Cross Flow, Combust. Flame 98 (1994) 267–278.

[35] A. Palacios, D. Bradley, Qiang Wang, Xin Li, Longhua Hu, Air/fuel Mixing in Jet Flames. Submitted for publication.

[36] A. Palacios, J. Casal, D. Bradley, Prediction of Lift-Off Distance in Choked and Subsonic Hydrogen Jet Fires, Catal. Today (2019) 221–224.

[37] W. Ockwig, T.M. Nenoff, Membranes for Hydrogen Separation, Chem. Rev. 107 (2007) 4078–4110.